

## Achievable Dynamic Performance in Telerobotic Systems

Peter M. Bobgan, H. Kazerooni

Mechanical Engineering Department  
University of Minnesota, Minneapolis, MN 55455

### Abstract

The work presented here defines a control algorithm for a telerobotic system in which the dynamic behaviors of the slave robot and the master robot are functions of each other. These functions, which are the designer's choice and depend on the application, are described. A control architecture is then presented which guarantees that the specified functions govern the dynamic behavior of the telerobotic system. The stability of the closed-loop system (i.e., master robot, slave robot, human, and the load being manipulated) is analyzed and sufficient conditions for stability are derived. A set of experiments is given to verify the theoretical predictions.

### 1. The Telerobotic Control Specifications

Figure 1 shows a telerobotic system which is used to manipulate an object through a completely arbitrary trajectory. The goal may be a dynamic behavior in which the human senses scaled-down values of the forces that the slave senses when manipulating the object. Therefore, a controller must be designed so that the ratio of the forces on the slave to the forces on the master equals a number greater than unity. If  $f_s$  and  $f_m$ <sup>1</sup> represent the forces on the slave and on the master, then  $f_s = -\alpha f_m$  where  $\alpha$  is a scalar greater than unity. (The negative sign, originating from the convention used in Figure 1, implies the opposite directions of  $f_s$  and  $f_m$ .) Furthermore, if the object being manipulated is a pneumatic jackhammer, the goal may be to both filter and decrease the jackhammer forces. Then, the human senses only the low-frequency, scaled-down components of the forces that the slave senses. This requires a low-pass filter such that  $f_s = -\alpha f_m$  where  $1/\alpha$  is a low-pass filter transfer function.

In addition to scaling the forces, one may require a behavior for the telerobotic system in which the slave robot position equals a scaled-down value of the master robot position. In other words, if  $y_s$  and  $y_m$  are

the positions of the slave robot and the master robot, then  $y_s = \beta y_m$  where  $\beta$  is smaller than unity. This behavior is useful when great precision is required in the slave maneuver; a few centimeters of master motion correspond to a few microns of slave motion.

Without formal proof, it is stated that, for linear systems, only three independent relationships can be specified among the four variables:  $y_m$ ,  $y_s$ ,  $f_m$ , and  $f_s$ . One possible set of relationships is:

$$y_s = A_y y_m, \quad (1)$$

$$f_s = A_f f_m, \quad (2)$$

$$f_s = Z_s y_s. \quad (3)$$

$A_y$ ,  $A_f$ , and  $Z_s$  are transfer functions.  $A_y$  and  $A_f$  represent the relationships between the positions and forces while  $Z_s$  is the slave port impedance. Note that, once the above three relationships are specified, no other independent relationships can be specified.

"Telepresence" discussed in recent literature, specifies a dynamic behavior in which the environmental effects experienced by the slave are transferred through the master to the human without alteration; therefore, the human feels that she/he is "there" without "being" there [2, 3, 4, 10, 12].

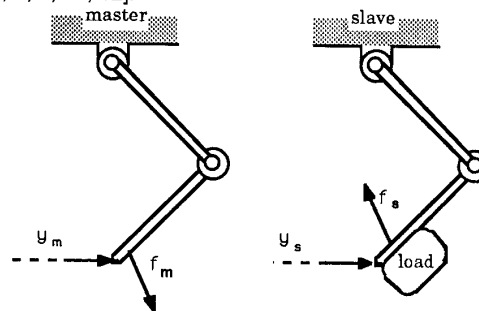


Figure 1: In telerobotic system, human constrains master robot motion while environment constrains slave robot motion.

In contrast with telepresence, the above design specifications allow the designers to alter the

<sup>1</sup> The subscript "m" signifies the master and "s" signifies the slave.

environmental effects on the human. Note, these design specifications are independent of the chosen control architecture and do not assure stability. The next section however, introduces a new and practical control architecture which achieves the design specifications and guarantees stability.

## 2. The Control Architecture

The proposed control architecture lets designers handle the robustness of the master robot and the slave robot without getting involved in the dynamics of the human, the dynamics of the object being manipulated by the slave, or the communication time delay [1]. The control architecture design must include the dynamic behavior of the master robot, slave robot, human arm and load being maneuvered.

### Dynamic Behaviors of the Master and Slave Robots

Each robot has a closed-loop velocity controller. Throughout this article, this controller is called a *primary stabilizing controller*. The resulting closed-loop system is called a *primary closed-loop system*. The following motivated our choosing a closed-loop primary stabilizing controller for the robots:

1. A closed-loop velocity control system (usually referred to as rate control) eliminates the effects of frictional forces in the joints and in the transmission mechanism, and creates a more definite dynamic behavior in the robots. Minimizing the effects of uncertainty in the system is a usual design specification for velocity controllers.
2. A closed-loop velocity control system creates linear dynamic behavior in the robots. Here we assume that, for non-linear robot dynamics, a nonlinear stabilizing controller has been designed to yield a nearly linear closed-loop velocity system for the robot. See reference [13] for a nonlinear analysis of the dynamics and control of robotics.
3. Choosing a closed-loop velocity system for the robots lets the designers deal with the robot robustness without knowledge of the human or environment dynamics. These dynamics which change with each operator and environment can be considered separately.
4. Human safety dictates that the master robot remain stable when not worn by a human. A closed-loop velocity control system keeps the robot stationary when not being maneuvered.

Only the master robot dynamic behavior is derived here; the derivation of the slave robot dynamic behavior is similar to that of the master robot. The master robot velocity,  $v_m$ , results from two inputs:  $u_m$ , the electronic command to the primary controller of the master robot and  $f_m$ , the forces imposed on the master robot. The transfer function  $G_m$  is defined as the primary closed-loop system and has the electronic command  $u_m$  as input and the master velocity,  $v_m$ , as output. The master robot sensitivity transfer function,  $S_m$ , maps the force imposed on the master robot,  $f_m$ , onto the master

velocity,  $v_m$ . Equation 4 represents the master robot dynamic behavior in its most general form:

$$v_m = G_m u_m + S_m f_m. \quad (4)$$

Since the master robot is maneuvered by the human,  $f_m$  represents the human contact forces. The motion of the master robot has a small response to the human forces,  $f_m$ , if the magnitude of  $S_m$  is small. A small  $S_m$  results when the primary stabilizing controller is a high-gain closed-loop velocity controller or when the actuator has a high gear ratio [5].

Note that  $G_m$  and  $S_m$  depend on the nature of the primary stabilizing controller. In particular, they vary depending on the particular compensator chosen for the closed-loop velocity system. If a compensator with several integrators is chosen to ensure small steady state errors, then  $S_m$  will be small in comparison to  $G_m$ . If the robot actuators are non-backdrivable, then  $S_m$  will be small regardless of how carefully the robot's primary compensator is chosen.

Similarly, the dynamic behavior of the slave robot is defined by equation 5:

$$v_s = G_s u_s + S_s f_s. \quad (5)$$

$f_s$  is the force imposed by the environment on the slave endpoint, and  $u_s$  is the input command to the primary controller of the slave drive system.  $G_s$  and  $S_s$  are similar to  $G_m$  and  $S_m$ , and represent the effects of  $u_s$  and  $f_s$ .

### Dynamic Behavior of the Human Arm

In this work, the human arm is modeled as a non-ideal force control system. The force imposed by the human arm on the master robot results from two inputs. The first input,  $u_h$ , is a force imposed by the human muscles<sup>2</sup>. The second input is the position of the master robot. Thus, the master robot motion can be thought of as a position disturbance occurring on the force-controlled human arm. If the master robot is stationary, the force imposed on the master robot is a function of human muscle forces. If the master robot moves, the force imposed on the master robot is a function not only of the muscle forces but also of the master robot position. Therefore, the force imposed on the master robot is different from  $u_h$ . The transfer function  $S_h$  maps the master robot position,  $y_m$ , into the force imposed on the master robot,  $f_m$ :

<sup>2</sup> It is assumed that the specified form of  $u_h$  is not known other than that it is the result of human thought deciding to impose a force onto the master robot [11, 14]. The dynamic behavior in the generation of  $u_h$  by the human central nervous system is of little importance in this analysis since it does not affect the system performance and stability.

$$f_m = U_h - S_h Y_m . \quad (6)$$

$S_h$ , the human arm sensitivity function (or impedance [6, 7]), is the disturbance rejection property of the human arm. If the gain of  $S_h$  is small, the master robot motion has a small effect on the imposed forces,  $f_m$ .

#### Dynamic Behavior of the Environment

Telerobotic systems are used for manipulating objects or imposing forces on objects.  $E$  is a transfer function which represents the environment dynamics and  $f_{ext}$  is the sum of all external forces imposed on the environment. Equation 7 provides a general expression for the force imposed on the slave robot in the linear domain<sup>3</sup>:

$$f_s = - E Y_s + f_{ext} . \quad (7)$$

If the slave robot is employed for pushing a spring and damper, then  $E$  is a transfer function such that  $E(s) = (K + Cs)$  and  $f_{ext} = 0$  where  $K$ ,  $C$ ,  $Y_s$ , and  $s$  are the stiffness, damping, slave position, and Laplace operator. In another example, if the slave robot is employed for maneuvering a mass, then  $E(s) = J s^2$  where  $J$  is the inertia of the object.

The dynamic behavior of the telerobotic system, the human arm, and the environment is represented by the block diagram in Figure 2 which uses equations 4, 5, 6, and 7 as the dynamic models of the master robot, the slave robot, the human arm, and the environment. In the diagram,  $H$  is the control feedback operating on the contact forces. Note that there is no cross-feedback between the positions; only the forces are measured for feedback. This is a fundamental difference between this control method and previous control methods.

In Figure 2, if  $U_s$ ,  $U_m$ ,  $U_h$ , and  $f_{ext}$  are zero (i.e., the inputs to the master robot and the slave robot are zero, the human has no intention of moving the master robot, and no other forces are imposed on the slave) and  $H_{11}$  and  $H_{21}$  are chosen to be zero, the interaction force between the human and the master is zero. If the human decides to move her/his hand (i.e.,  $U_h$  becomes a nonzero value) and  $U_m$ ,  $U_s$ ,  $f_{ext}$ ,  $H_{11}$ , and  $H_{21}$  are still zero, the physical contact between the human and the master robot produces some master robot motion as  $f_m$  acts through  $S_m$ . In general,  $S_m$  is very small; thus, the human operator alone does not have sufficient strength to move the master robot as desired.

<sup>3</sup>  $f_{ext}$  can be thought of as the equivalent of all the forces on the slave robot endpoint which do not depend on  $Y_s$  and other system variables. One example of  $f_{ext}$  can be observed when a second human is holding and maneuvering the slave endpoint; the force imposed on the slave endpoint by the human represents  $f_{ext}$ . In this article it is assumed that  $f_{ext} = 0$ .

An additional route for  $f_m$  to map to  $Y_m$  can be added if  $H_{11}$  is chosen to be non-zero; The interaction force  $f_m$  is measured and filtered by compensator  $H_{11}$  and then used as an input to the master robot's primary controller. Note that the mapping  $G_m H_{11}$  acts in parallel to  $S_m$  and thus increases the apparent sensitivity of the master robot.  $G_m$  and  $S_m$  are fixed by the mechanical design of the master robot and by the chosen primary stabilizing controller. However, the designer can adjust the apparent sensitivity along the path from  $f_m$  to  $Y_m$  using  $H_{11}$ . At this point, there is no restriction placed on the structure and size of  $H_{11}$ , but figure 2 suggests choosing a large gain for  $H_{11}$  to increase the apparent sensitivity of the master robot. The interaction force  $f_m$  is also used to drive the slave robot after passing through the compensator  $H_{21}$ . If  $H_{11} = H_{21}$ , the master and slave motion are the same.

Similarly, compensator  $H_{22}$  is chosen to generate compliancy in the slave robot in response to the forces,  $f_s$ , imposed on the slave robot endpoint [5, 9]. The interaction force  $f_s$  also affects the master robot as a force reflection after passing through the compensator  $H_{12}$ .

The goal is to find the  $H$  transfer function matrix such that the satisfaction of equations 1, 2, and 3 is guaranteed for the system. But, designers do not have complete freedom in choosing the structure and magnitude of  $H$  because the closed-loop system must remain stable for any chosen  $H$ .

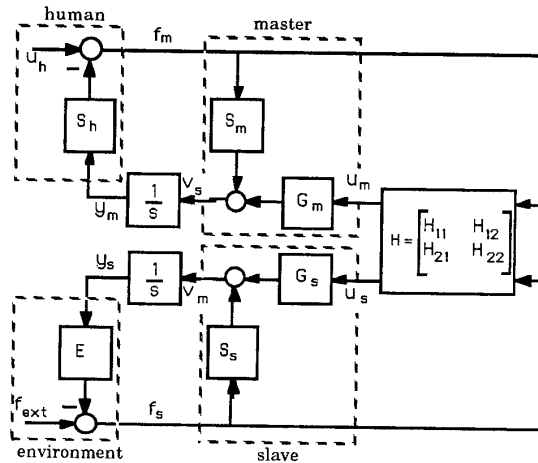


Figure 2: The proposed control architecture .



$$\text{if } S_h P_{11} + 1 \neq 0 \quad \forall \omega \in [0, \infty) \quad (23)$$

Then, dividing 22 by 23 results in:

$$1 + \frac{(S_h \delta P + P_{22})E}{S_h P_{11} + 1} \neq 0 \quad \forall \omega \in [0, \infty) \quad (24)$$

To ensure the truth of 24, one must guarantee that:

$$\left| \frac{(S_h \delta P + P_{22})E}{S_h P_{11} + 1} \right| < 1 \quad \forall \omega \in [0, \infty) \quad (25)$$

Therefore, to ensure the stability of the system in Figure 3, inequalities 25 and 23 must be guaranteed; these inequalities are restated as follows:

$$\left| \frac{1 + P_{11} S_h}{P_{22} + \delta P S_h} \right| > |E| \quad \forall \omega \in [0, \infty) \quad (26)$$

$$|P_{11}| < \frac{1}{|S_h|} \quad \forall \omega \in [0, \infty) \quad (27)$$

Comparing inequality 26 with equation 11 shows that the left-hand side of equation 26 equals  $Z_s$ . The stability conditions in inequalities 27 and 26 can be satisfied easily because the left-hand sides of these inequalities are the designers' choice:  $Z_s$  must be larger than  $E$  and  $P_{11}$  must be smaller than  $1/S_h$  in magnitude. This presents an interesting property of the proposed control law: the stability criteria (inequalities 27 and 26) do not limit the designer in choosing  $A_f$  and  $A_y$ , but only restrict the designer in choosing  $Z_s$ . To summarize, designers can choose three functions  $A_f$ ,  $A_y$ , and  $Z_s$  to describe the system behavior; while there is no restriction on the choice of  $A_f$  and  $A_y$ ,  $Z_s$  (slave impedance) must be larger than  $E$ .

## 6. Experiments

The one-degree-of-freedom telerobotic system shown in Figure 3 is used to verify the performance of the system when the goal is to shape the forces. The master robot is a link powered by a DC motor. The human holds the handle on the link to maneuver the master robot, and a force sensor between the handle and the link measures the human contact force. The slave robot is also a link powered by a DC motor. A mass representing a load is attached to the slave link, and a force sensor between the load and the link measures the load force. (The detailed drawings of the force sensor assembly have been omitted for brevity.) Two independent primary stabilizing controllers for the master robot and for the slave robot have been designed to yield the widest bandwidth for the closed-loop transfer functions,  $G_m$  and  $G_s$ , while guaranteeing the stability of each system in the presence of bounded unmodeled dynamics. The dominant dynamics for  $G_m$  and  $G_s$  representing the

closed-loop velocity system are given by equation 28. (The development of the velocity controllers for both robots has been omitted for brevity.)

$$G_m = G_s = \frac{0.95}{0.02 s + 1} \quad \frac{\text{rad/sec}}{\text{rad/sec}} \quad (28)$$

The link on each robot is driven through an 80:1 harmonic drive. This large reduction ratio in conjunction with the closed-loop velocity controller results in stiff systems with very small sensitivity transfer functions:  $S_m$  and  $S_s$ . The DC values of  $S_m$  and  $S_s$  are:

$$S_m = S_s = 0.01 \quad \text{rad/sec /ft.lbf} \quad (29)$$

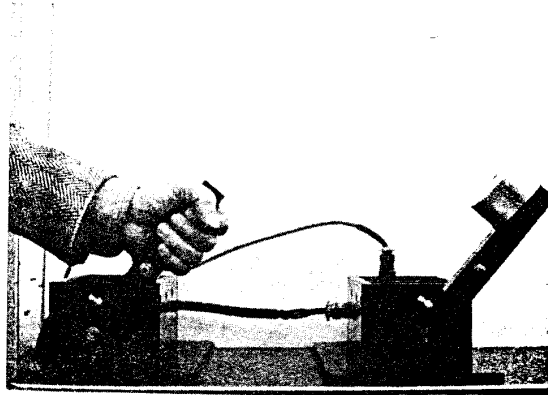


Figure 4: One-Degree-of-Freedom Experimental Telerobotic System

The slave robot is employed to maneuver a mass such that:

$$E = J s^2 \quad \text{lbf/rad.} \quad (30)$$

where  $J = 0.05 \text{ ft.lbf.sec}^2$  is the moment of inertia.

The objective of the experiment is to verify the proposed control architecture in achieving the performance specifications described by equations 1, 2 and 3. In the experiment, a number of controllers are designed each with a different combination of  $A_f$  and  $A_y$  specifications. We only specify  $A_f$  and  $A_y$  without any restriction on  $Z_s$ . We choose  $\delta P$  to be zero and use equations 8 and 9 to solve for  $P_{12}$ ,  $P_{21}$ , and  $P_{22}$  in terms of  $P_{11}$  which is an arbitrary choice.

$$P_{21} = P_{11} A_y, \quad (31)$$

$$P_{22} = -(P_{21} E + A_f) / A_f E, \quad (32)$$

$$P_{12} = P_{22} / A_y, \quad (33)$$

Equations 12-15 are used to calculate the elements of  $H$  assuming  $S_s$  and  $S_m$  are very small in comparison to other variables, and  $G_s$  and  $G_m$  are approximately unity

within the system bandwidth. Choosing  $P_{11} = K/s^2$  results in:

$$H_{11} = \frac{K}{s} \quad (34)$$

$$H_{12} = -\frac{K A_y J + A_f}{A_f A_y^2 J s} \quad (35)$$

$$H_{21} = \frac{K A_y}{s} \quad (36)$$

$$H_{22} = -\frac{K A_y J + A_f}{A_f A_y J s} \quad (37)$$

where  $K$  is chosen to guarantee the stability condition given by inequality 27. The controller is implemented and the system is maneuvered irregularly by an operator for 5.5 seconds. The motion generated by the operator can be thought of as a random function with low frequency components which fall within the bandwidth of the system. In the first set of experiments,  $A_y$  and  $-A_f$  are chosen to be unity. Figure 5 shows the slave position versus the master position where the near unity slope confirms the equality of master and slave positions for all low frequency components of the motion. Figure 6 shows  $-f_s$  versus  $f_m$  where the near unity slope confirms that the operator and slave force are nearly equal.

In another set of experiments,  $A_y$  and  $-A_f$  are chosen to be 1 and 3 respectively. Figure 7 shows the slave position versus the master position where the near unity slope confirms the equality of master and slave positions for all low frequency components of the motion. Figure 8 shows  $-f_s$  and  $f_m$  where the human feels a scaled down value of the slave force.

In the last set of experiments,  $A_y$  and  $-A_f$  are chosen to be 0.5 and 1 respectively; scaling-down the slave position by factor of 2. Figure 9 shows the slave and master position where the slave position is one half of the master position. Figure 10 shows  $-f_s$  vs  $f_m$  where the near unity slope confirms the equality of master and slave forces for all low frequency components of the motion.

## 7. Summary and Conclusion

This article introduces the design specifications for telerobotic control systems. A minimum number of functions are defined to frame the telerobotic specifications. The stability of the system (i.e., master robot, slave robot, human, and the load being manipulated) is analyzed and sufficient conditions for stability are derived. A set of experimental results are given to verify the theoretical claims.

## 8. References

- 1) Anderson, R. J., Spong, M. W., "Asymptotic Stability for Force Reflecting Teleoperators with Time Delay", IEEE Int. Conf. on Robotics and Automation, Scottsdale, AZ, May 1989.
- 2) Bejczy, A. K., Handlykken, M., "Experimental Results with a Six Degree-of-Freedom Force

- Reflecting Hand Controller," in Proc. 17th Annual Conference on Manual Control, Los Angeles, CA, June 1981.
- 3) Bejczy, A. K., Bekey, G., Lee, S. K., "Computer Control of Space Borne Teleoperators with Sensory Feedback," IEEE Conference on Robotics and Automation, 1985.
- 4) Hannaford, B., "A Design Framework for Teleoperators with Kinematic Feedback", IEEE Trans. on Robotics and Automation, Vol 5, No 4, August 1989.
- 5) Kazerooni, H., "On the Robot Compliant Motion Control," ASME J. of Dyn. Systems, Measurement, and Control, Vol. 111, No. 3, September 1989.
- 6) Kazerooni, H., "Human-Robot Interaction via the Transfer of Power and Information Signals", IEEE Trans. on Systems and Cybernetics, Vol 20, No 2, March 1990.
- 7) Kazerooni, H., Meidt, J. D., "On the Stability and Performance of Robotic Systems Worn by Humans", IEEE International Conference on Robotics and Automation, Cincinnati, OH, May 1990.
- 8) Lehtomaki, N.A., Sandell, N.R., Athans, M., "Robustness Results in Linear-Quadratic Gaussian Based Multivariable Control Designs", IEEE Trans. on Automatic Control AC-26(1):75-92, February 1981.
- 9) Mason, M.T., "Compliance and Force Control for Computer controlled Manipulators", IEEE Transactions on Systems, Man and Cybernetics SMC-11(6):418-432, June 1981.
- 10) Raju, G. J., Verghese, G. C., Sheridan, T. B., "Design Issues in 2-port Network Models of Bilateral Remote Manipulation", IEEE Int. Conference on Robotics and Automation, Scottsdale, AZ, May 1989.
- 11) Repperger, D. W., Morris, A., "Discriminant Analysis of Changes in Human Muscle Function When Interacting with an Assistive Aid", IEEE Transactions on Biomedical Engineering, Vol 35, No 5, May 1988.
- 12) Sheridan, T. B., "Telerobotics", in the Proceedings of the Workshop on Shared Autonomous and Teleoperated Manipulator Control, Philadelphia, PA, 1988.
- 13) Spong, M.W., Vidyasagar, M., "Robust Non-Linear Control of Robot Manipulators", IEEE, Conference on Decision and Control, December 1985.
- 14) Stein, R. B., "What muscles variables does the nervous system control in limb movements?", J. of the behavioral and brain sciences, Vol 5, pp 535-577, 1982.

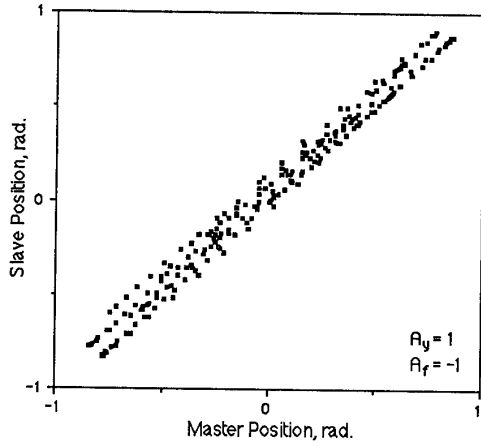


Figure 5:  $y_s$  vs  $y_m$  when  $A_y = 1$  and  $A_f = -1$

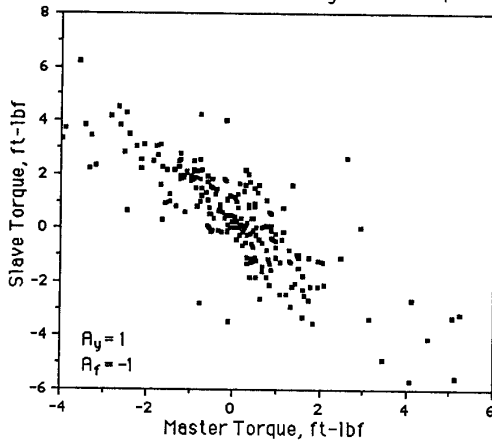


Figure 6:  $f_s$  vs  $f_m$  when  $A_y = 1$  and  $A_f = -1$

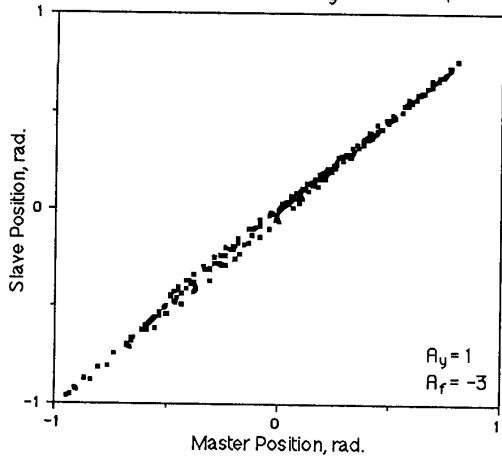


Figure 7:  $y_s$  vs  $y_m$  when  $A_y = 1$  and  $A_f = -3$

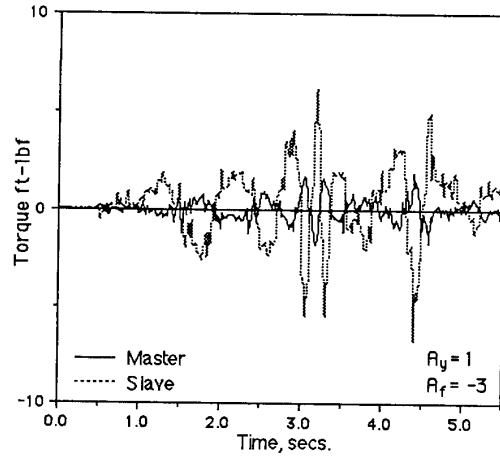


Figure 8:  $f_s$  and  $f_m$  when  $A_y = 1$  and  $A_f = -3$

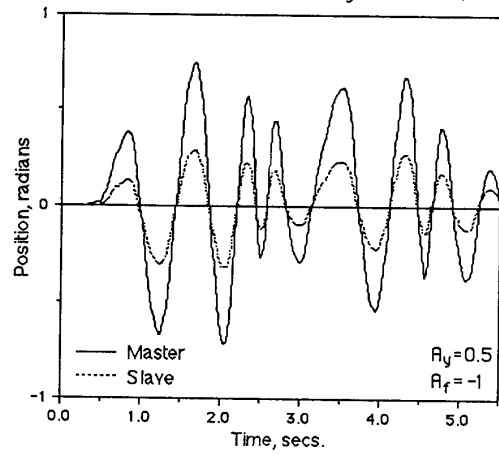


Figure 9:  $y_s$  and  $y_m$  when  $A_y = 0.5$  and  $A_f = -1$

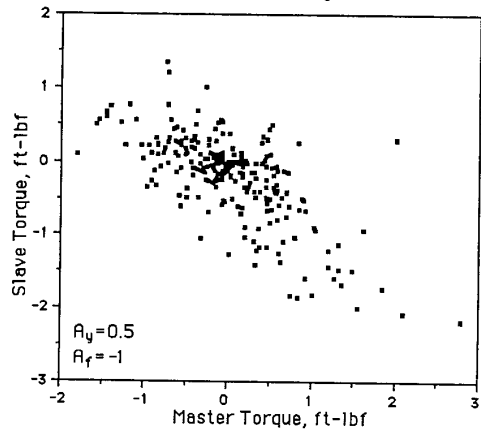


Figure 10:  $f_s$  and  $f_m$  when  $A_y = 0.5$  and  $A_f = -1$